Cluster-Assisted Thermal Energy Activation of the H−H σ Bond in H_2 by Ground State $B^+(^1S_0)$ Ions: Overcoming a 77 kcal/mol Barrier

Paul R. Kemper, John E. Bushnell, Patrick Weis, and Michael T. Bowers*

Contribution from the Department of Chemistry, University of California, Santa Barbara, California 93106

Received November 20, 1997. Revised Manuscript Received June 15, 1998

Abstract: Binding energies for the sequential addition of two dihydrogen ligands to ground-state $B^+(^1S_0)$ ions have been measured with use of equilibrium methods. The dissociation energies at 0 K were determined to be 3.8 and 3.0 kcal/mol, respectively. Similar measurements on inserted $HBH^+(^1\Sigma_g^+$ ground state) ions yielded binding energies of 14.7 and 18.0 kcal/mol for the addition of the first two H_2 ligands. Injection of B^+ into a cell containing 5 Torr of H_2 near 100 K resulted in a BH_6^+ terminal ion that was not in equilibrium with the lower mass B^+, $B^+(H_2)$, and $B^+(H_2)_2$ species. The rate constant for formation of this BH_6^+ terminal ion was measured as a function of temperature and found to peak near 100 K, rapidly decreasing at higher and lower temperatures. This highly unusual behavior was successfully quantitatively modeled by assuming the following mechanism, $B^+ + 3H_2 \rightleftarrows B^+(H_2)_3 \xrightarrow{-o} HBH(H_2)_2^+$, where the third uninserted cluster could rearrange with a 0.52 ± 0.5 kcal/mol barrier to form the much lower energy inserted ion. High-level ab initio calculations (ref 17) found a barrier of 77 kcal/mol for this insertion process when ground-state B^+ reacts with a single H_2 molecule. Our experiments show that addition of two weakly bound H_2 ligands reduces the barrier to near zero. To confirm this result, large basis set DFT calculations were done to explore the reaction pathway. These calculations do, in fact, predict a near-zero barrier for insertion upon adding a third H_2 to ground-state $B^+(H_2)_2$ ions. This DFT result has recently been confirmed by high-level ab initio calculations published elsewhere (refs 29 and 30). Additional high-level ab initio calculations on the $B^+(H_2)_2$ clusters are reported here and provide quantitative agreement with the measured bond energies.

Introduction

The activation of σ bonds is the primary focus of chemical catalysis and is arguably one of the most important areas of industrial research. Of central importance is the use of transition metals in catalysis, and a major research target is the controlled activation of C−H and C−C bonds in alkanes due to their importance in the treatment of petrochemicals. The magnitude of this quest is such that the controlled activation of the C−H bond in methane has recently been listed as one of the modern holy grails in chemistry.[1] Central to this is the question of how the nearly degenerate s and d atomic orbitals on the transition metals conspire to activate σ bonds.[2] In neutral systems, for example, the s orbital is always occupied and usually doubly occupied. Since the s orbital is larger than the d orbitals,[3] especially for first row transition metals, this orbital occupancy leads to long-range repulsion between the metal and an approaching molecule. As a consequence, reaction of ground-state atomic first row metals is very slow or nonexistent.[4] Inorganic and organometallic chemists have found that the metal center can be activated by attaching strongly oxidizing ligands to it, resulting in a formally ionic electron configuration. This oxidation process preferentially removes s electrons and thus reduces repulsive interactions with incoming target molecules. Ligand attachment also can strongly perturb both the energy and ordering of metal centered excited states that often are crucial in the reaction chemistry being studied. While this overall process is qualitatively well understood,[5] it has been difficult to extract detailed mechanistic information on orbital involvement in σ-bond activation since obtaining such information requires both accurate experiment and accurate high level electronic structure calculations. The addition of bulky ligands, required for the experiment to proceed, restricts and often prevents effective use of the required level of theory.

One successful strategy has been to begin with singly oxidized M(I) positive ions since these species generally have only one or zero valence s electrons in their ground states. Consequently it has been possible to obtain numerous M^+−ligand bond energies with a variety of methods,[6,7] often with accuracies as great as ± 0.1 kcal/mol.[8] It was the success and accuracy of these methods that led our group to investigate the details of σ-bond activation by transition metal centers,[9] initially using measurement of kinetic energy release as a tool[10] but most recently applying equilibrium methods[8,11] and high-level electronic structure calculations.[11]

(1) Arndtsen, B. A.; Bergman, R. G.; Mobley, T. A.; Peterson, T. H. *Acc. Chem. Res.* **1995**, *28*, 154.

(2) For a recent review, see: Bauschlicher, C. W.; Langhoff, S. R.; Partridge, H. In *Organometallic Ion Chemistry*; Freiser, B. S., Ed.; Kluwer Academic Publishers: Boston, 1996; pp 47−88.

(3) See, for example: Barnes, L. A.; Rosi, M.; Bauschlicher, C. W. *J. Chem. Phys.* **1990**, *93*, 609. Desclaux, P. *At. Nuclear Data Tables* **1973**, *12*, 312.

(4) See, for example: Weisshaar, J. C. *Acc. Chem. Res.* **1993**, *26*, 213.

(5) Cotton, F. A.; Wilkinson, G. *Advanced Inorganic Chemistry*; Interscience: New York, 1971.

(6) Armentrout, P. B.; Kickel, B. L. In *Organometallic Ion Chemistry*; Freiser, B. S., Ed.; Kluwer Academic Publishers: Boston, 1996; pp 1−46.

(7) For a compilation of early work, see: Keesee, R. G.; Castelman, A. W. *J. Phys. Chem. Ref. Data* **1986**, *15*, 1011.

(8) See, for example: Kemper, P. R.; Bushnell, J.; von Helden, G.; Bowers, M. T. *J. Phys. Chem.* **1993**, *97*, 52.

(9) For a recent review see: van Koppen, P. A. M.; Kemper, P. R.; Bowers, M. T. In *Organometallic Ion Chemistry*; Freiser, B. S., Ed.; Kluwer Academic Press: Boston, 1996; pp 157−196.

S0002-7863(97)03975-9 CCC: $15.00
Published on Web 07/17/1998

Of most importance to the work to be reported here was the surprising discovery of what we call "cluster assisted σ-bond activation", shown schematically below for activation of the H−H bond in dihydrogen:

$$M^+ + H_2 \not\rightarrow HMH^+$$

$$M^+ + nH_2 \rightarrow HMH^+ + (n-1)H_2$$

When M is a first row transition series metal, only Sc^+ inserts into H_2 via this mechanism, whose details are given elsewhere.[12] All other first row metals simply form a series of dihydrogen clusters, $M^+(H_2)_n$, with $n \leq 6$.[8,11] The surprising aspect of the Sc^+ insertion process was that theory had predicted[13,14] an insertion barrier of ~17 kcal/mol for ground-state Sc^+ interacting with a single H_2 molecule. The key to a successful insertion in this system was selective stabilization by multiple H_2 attachment of a key excited state of Sc^+ located 31 kcal/mol above the ground state, eventually leading to insertion.

We have found evidence for a related mechanism in the σ-bond activation of the important C−H bond in CH_4 where activation occurs on the addition of the third CH_4 ligand to Ti^+, overcoming an 18 kcal/mol barrier.[15] Similarly both Zr^+ and Nb^+ appear to activate CH_4 by cluster assisted mechanisms,[16] although no estimates of the barriers are available. The detailed mechanisms of these processes are still under investigation.

In this paper we investigate the possibility that the B^+ ion can fully activate the H−H bond of dihydrogen. In this instance it will be the interplay of the s and p electrons that will be important, rather than the s and d electrons of the transition metals. This is an appealing system since it is amenable to very high level ab initio and/or DFT calculations. In fact an ab initio study of the reaction of B^+ with H_2 to form HBH^+ has been carried out.[17] The calculations indicate the insertion reaction itself is strongly exoergic (>40 kcal/mol) but is prevented from occurring for ground-state, thermal energy B^+ ions by a very high barrier (>50 kcal/mol), a result consistent with ion beam experimental results.[18] The origin of the barrier is the very high energy of the $^1P(2s2p)$ excited state that correlates to the inserted product (the ^1P state lies over 200 kcal/mol above the $^1S(2s^2)$ ground state of B^+). Hence, this system provides a real challenge for the cluster assisted σ-bond activation mechanism that has been successful for a number of transition metals where barriers to reaction were at much lower energies.

DePuy and co-workers[19] have investigated reactions of B^+ with H_2 in a selected ion flow tube. Under their experimental conditions no reaction was observed (300 K, 0.5 Torr). This result is consistent with the ab initio predictions.[17] However, they did observe rapid addition of two dihydrogen molecules to HBH^+ when this species was injected into the flow tube. Their calculations[19] indicated that HBH^+ binds two H_2 ligands strongly, a prediction consistent with their observation.

In the present work we analyze the reactions of both B^+ and HBH^+ with H_2 over the temperature range of 80 to 675 K and obtain binding energies for multiple H_2 additions from temperature-dependent equilibrium studies. Evidence will also be presented for σ-bond activation of H_2 by dihydrogen ligated B^+ ions. These surprising results will be rationalized by high-level calculations and the detailed mechanism discussed. Our results follow.

Experimental Section

The details of the apparatus have been described previously[20] and will only be described briefly here. The ions used (B^+, BH_2^+, and BBr_2^+) are formed by electron impact on BBr_3 or B_2H_6 in the ion source. The particular ion of interest is then quadrupole mass selected and injected through a small hole (0.5 mm diameter) into a drift reactor containing between 3 and 10 Torr of H_2 gas. The ions are subjected to a small electric field that pulls them through the reactor and they eventually exit through a small hole. The ion distribution exiting the reactor is obtained by scanning a second quadrupole mass filter. Ion injection energies can be varied from a few to hundreds of electronvolts (lab). Typically 10 eV was used in these studies unless otherwise stated. The drift reactor is temperature variable from 80 to 800 K.

Equilibrium constants were obtained for reactions of the type

$$B^+(H_2)_{n-1} + H_2 \rightleftarrows B^+(H_2)_n \quad (1)$$

$$HBH^+(H_2)_{m-1} + H_2 \rightleftarrows HBH^+(H_2)_m \quad (2)$$

over a wide range of temperatures. The usual checks were made to ensure equilibrium was obtained by varying the reaction time and the H_2 pressure by over at least factors of 2 and ensuring the equilibrium constant was unchanged within experimental error. The ΔG_T° for a reaction was obtained from eq 3

$$\Delta G_T^\circ = -RT \ln K_{eq} \quad (3)$$

and the underlying values of ΔH_T° and ΔS_T° obtained from eq 4

$$\Delta G_T^\circ = \Delta H_T^\circ - T\Delta S_T^\circ \quad (4)$$

by obtaining ΔG_T° at a series of temperatures; the 0 K intercept is ΔH_0° and the slope yields ΔS_T°.

One concern was the electronic state of the B^+ ions formed by electron impact. Long-lived metastable states are often formed in this process and can be very difficult to deactivate.[8,21] For this reason, the state distribution was probed with use of the ion chromatography method.[22,23] In this experiment 5 Torr of He is placed in the drift reactor and a short pulse (1−5 μs) of B^+ ions injected. An arrival time distribution (ATD) is then measured at the detector. Such an experiment for B^+ ions formed by 250 eV electron impact on BBr_3 is given in Figure 1a where the B^+ peak was injected at low energy. Two peaks are observed, a large one at ~90 μs and a small one (of 6 or 7% abundance) at ~120 μs. The large peak is almost certainly due to the $2s^2(^1S)$ ground-state B^+ ions and the small peak at longer times to the

(10) van Koppen, P. A. M.; Jacobson, D. B.; Illies, A. J.; Bowers, M. T.; Hanratty, M. A.; Beauchamp, J. L. *J. Am. Chem. Soc.* **1989**, *111*, 1991. Hanratty, M. A.; Beauchamp, J. L.; Illies, A. J.; van Koppen, P. A. M.; Bowers, M. T. *J. Am. Chem. Soc.* **1988**, *110*, 1. van Koppen, P. A. M.; Bowers, M. T.; Beauchamp, J. L.; Dearden, D. V. In *Bonding Energetics in Organometallic Compounds*; Marx, T. J., Ed.; ACS Symp. Ser. 428; American Chemical Society: Washington, DC, 1990.

(11) Bushnell, J. E.; Mâitre, P.; Kemper, P. R.; Bowers, M. T. *J. Chem. Phys*. **1997**, *106*, 10153 and references therein.

(12) Bushnell, J. E.; Kemper, P. R.; Mâitre, P.; Bowers, M. T. *J. Am. Chem. Soc.* **1994**, *116*, 9710.

(13) Alvarado-Swaisgood, A. E.; Harrison, J. F. *J. Phys. Chem.* **1985**, *89*, 5198.

(14) Rappé, A. K.; Upton, T. H. *J. Chem. Phys.* **1986**, *85*, 4400.

(15) van Koppen, P. A. M.; Bushnell, J. E.; Kemper, P. R.; Bowers, M. T. *J. Am. Chem. Soc.* **1995**, *117*, 2098.

(16) van Koppen, P. A. M.; Bushnell, J. E.; Bowers, M. T. Unpublished data.

(17) Nichols, J.; Gutowski, M.; Cole, S. J.; Simons, J. *J. Phys. Chem.* **1992**, *96*, 644.

(18) Lin, K. C.; Watkins, H. P.; Cotter, R. J.; Koski, W. S. *J. Chem. Phys.* **1974**, *56*, 1003. Ruatta, S. A.; Hanley, L.; Anderson, S. L. *J. Chem. Phys.* **1989**, *91*, 226. Armentrout, P. B. *Int. Rev. Phys. Chem.* **1990**, *9*, 115.

(19) DePuy, C. H.; Gareyev, R.; Hankin, J.; Davico, G. E.; Damrauer, R. *J. Am. Chem. Soc.* **1997**, *119*, 427.

(20) Kemper, P. R.; Weis, P.; Bowers, M. T. *Int. J. Mass Spectrom. Ion Proc.* **1997**, *160*, 17.

(21) von Helden, G.; Kemper, P. R.; Hsu, M.-T.; Bowers, M. T. *J. Chem. Phys.* **1992**, *96*, 6591.

(22) Kemper, P. R.; Bowers, M. T. *J. Phys. Chem.* **1991**, *95*, 5134.

(23) Bowers, M. T.; Kemper, P. R.; von Helden, G.; van Koppen, P. A. M. *Science* **1993**, *260*, 1446.

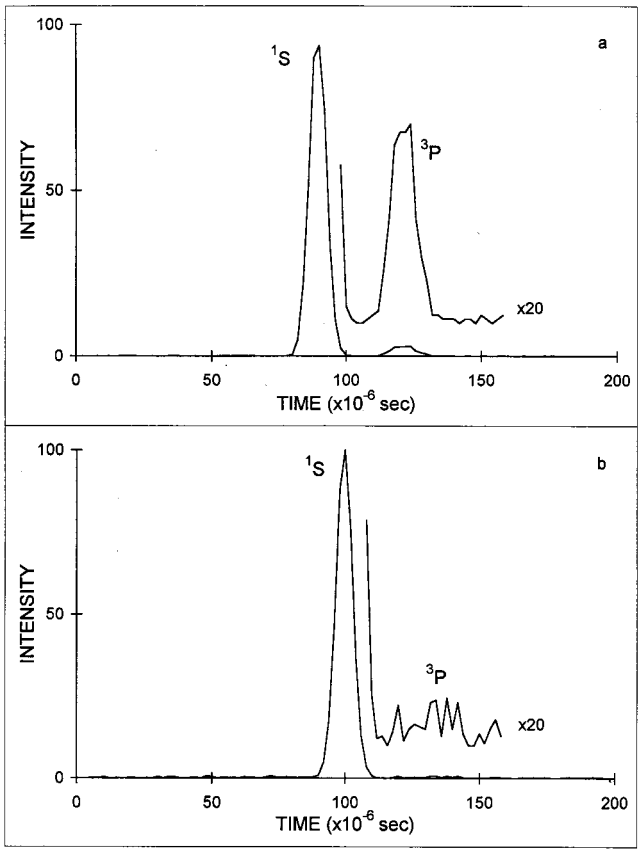

Figure 1. Arrival time distributions for B^+ ions injected into the drift cell containing 5 Torr of He at 300 K. (a) B^+ formed by 250 eV electron impact on BBr_3 in the ion source and injected at 10 eV (lab). The assignments to the electronic states of B^+ are given. (b) BBr_2^+ injected at 300 eV (lab) creating B^+ by collision induced dissociation. The peak labeled ^{3}P in panel a is not present above the noise level. A slightly smaller drift voltage was used than in panel a accounting for the small shift to longer times in the ^{1}S peak.

$2s2p(^3P)$ metastable first excited state 106 kcal/mol above the ground state. For transition metals, a $4s3d^{n-1}$ electron configuration had an arrival time ~50% shorter than the same metal ion with a $3d^n$ configuration, a result consistent with the above assignment. One way to test this assumption is to inject molecular ions at high energy, collisionally dissociate them, and measure the arrival time distribution of the resulting B^+ ion. This was done for BBr^+ ions injected at 300 eV (lab) with the results given in Figure 1b. In this instance only the larger short time peak remains (the peak assigned to the ^{3}P metastable is now less than 0.5% of the total intensity). All equilibria reported here that were initiated with B^+ ions were done by injecting high-energy BBr^+ ions into a high pressure of H_2, eliminating any complications due to excited states.

Finally, $^{10}B^+$ and $^{11}B^+$ isotopes were both used for all experiments and essentially identical results were obtained.

Results

Experiment. Equilibrium constants were measured over a range of temperatures for sequential addition of up to two H_2 molecules to B^+ and HBH^+ (eqs 1 and 2). Plots were made of ΔG_T° versus T (eqs 3 and 4) and their results given in Figure 2. The temperature range over which equilibrium could be followed for H_2 addition to B^+ was 110 to 350 K while H_2 addition to HBH^+ was found to be in equilibrium from 350 to 675 K. These data immediately indicate that H_2 is weakly bound to the B^+ ion and more strongly bound to the HBH^+ core ion. This observation is born out in the values of ΔH_T° extracted from the data by linear extrapolation to 0 K and collected, along with ΔS_T°, in Table 1.

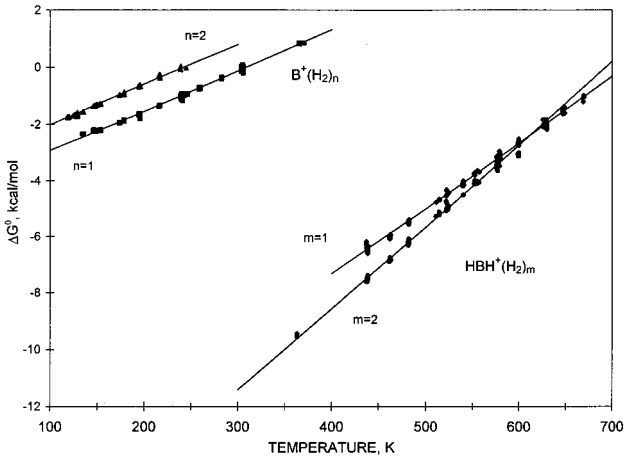

Figure 2. A plot of ΔG_T° vs temperature for the reactions $B^+(H_2)_{n-1} + H_2 \rightleftarrows B^+(H_2)_n$ and $HBH^+(H_2)_{m-1} + H_2 \rightleftarrows HBH^+(H_2)_m$ for $n = 1$, 2 and $m = 1$, 2.

Table 1. Experimental ΔH_T° and ΔS_T° for the Equilibrium

$$B^+(H_2)_{n-1} + H_2 \rightleftarrows B^+(H_2)_n$$

$$HBH(H_2)^+_{m-1} + H_2 \rightleftarrows HBH(H_2)^+_m$$

	ΔH_T°, kcal/mol	ΔS_T°, cal/(mol·K)	temp range, K
$n =$			
1	4.3 ± 0.1	14.0 ± 1.5	125−360
2	3.4 ± 0.2	14.3 ± 1.5	115−235
$m =$			
1	16.7 ± 0.4	23.4 ± 2.0	425−660
2	20.3 ± 0.4	29.2 ± 2.0	350−650

Table 2. Values of the Binding Energies ($-\Delta H_0^\circ$) in kcal/mol for the Listed Reactions

reaction	expt	ab initio QCISD(T)[a]	DFT[b]
$B^+ + H_2 \rightarrow B^+(H_2)$	3.8 ± 0.2	3.1	6.8
$B^+(H_2) + H_2 \rightarrow B^+(H_2)_2$	3.0 ± 0.3	2.5	5.0
$B^+(H_2)_2 + H_2 \rightarrow B^+(H_2)_3$		2.3	2.5[c]
$B^+(H_2)_3 + H_2 \rightarrow B^+(H_2)_4$		1.9	
$B^+(H_2)_4 + H_2 \rightarrow B^+(H_2)_5$		1.4	
$B^+(H_2)_5 + H_2 \rightarrow B^+(H_2)_6$		1.3	
$B^+ + H_2 \rightarrow HBH^+$		55.7	69
$HBH^+ + H_2 \rightarrow HBH^+(H_2)$	14.7 ± 0.5	13.8 (14.5)[d]	16.2
$HBH^+(H_2) + H_2 \rightarrow HBH^+(H_2)_2$	18.1 ± 0.5	16.2 (17.6)[d]	17.4

[a] With a 6-311++G(2df,p) basis set. [b] D95++(3df, 3pd) basis set. [c] D95++(d, p) basis set (see text). [d] Theoretical bond energies from ref 19. These calculations were done at the MP2(fu)/6-311G(d,p) level of theory.

The 0 K bond dissociation energies ($-\Delta H_0^\circ$) can be determined from the data in Figure 2 by extrapolating to 0 K with statistical mechanics. This extrapolation requires a knowledge of vibrational frequencies and rotational constants for all species. Since these are not known from experiment, theoretical values were used (next section). The resulting values of ΔH_0° are given in Table 2.

A set of initially puzzling observations were made while obtaining the equilibrium constants for H_2 addition to B^+. Examples of these are given in Figures 3 and 4. In Figure 3 a series of mass spectra are displayed obtained by injecting $^{11}BBr_2^+$ into H_2 at 300 eV. The cell temperature was held at 127 K. The top panel was taken with a drift time of 0.74 ms through the cell, the center panel with a drift time of 3.72 ms, and the bottom panel with a drift time of 7.36 ms. In all three panels the $B^+/B^+(H_2)$ and $B^+(H_2)/B^+(H_2)_2$ ratios are identical,

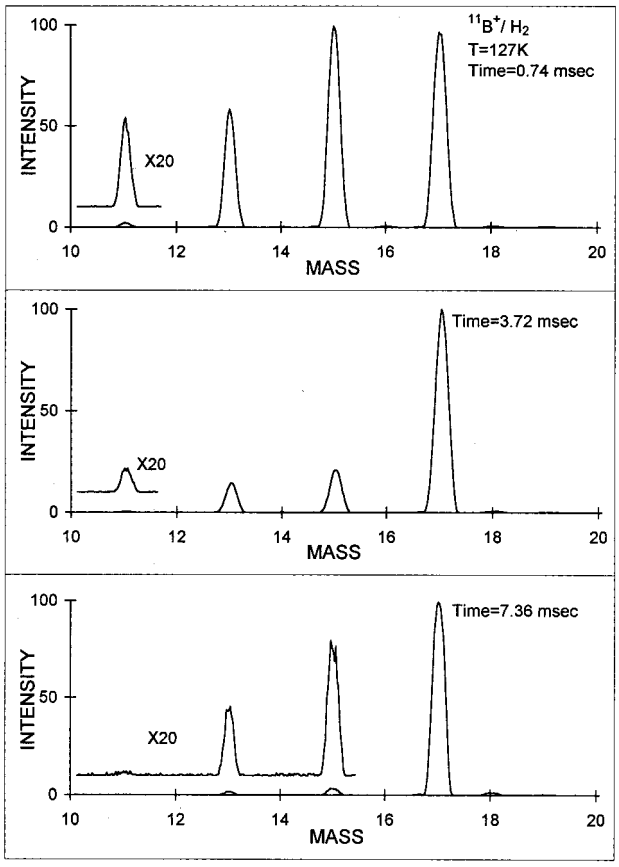

Figure 3. Mass spectra of ions exiting the drift reaction cell when $^{11}B^+$ was injected into 2.0 Torr of H_2 at 127 K. The top panel was for a drift time of 0.74 ms, the middle panel for 3.72 ms, and the bottom panel for 7.36 ms. In all cases the H_2 pressure was 2.0 Torr.

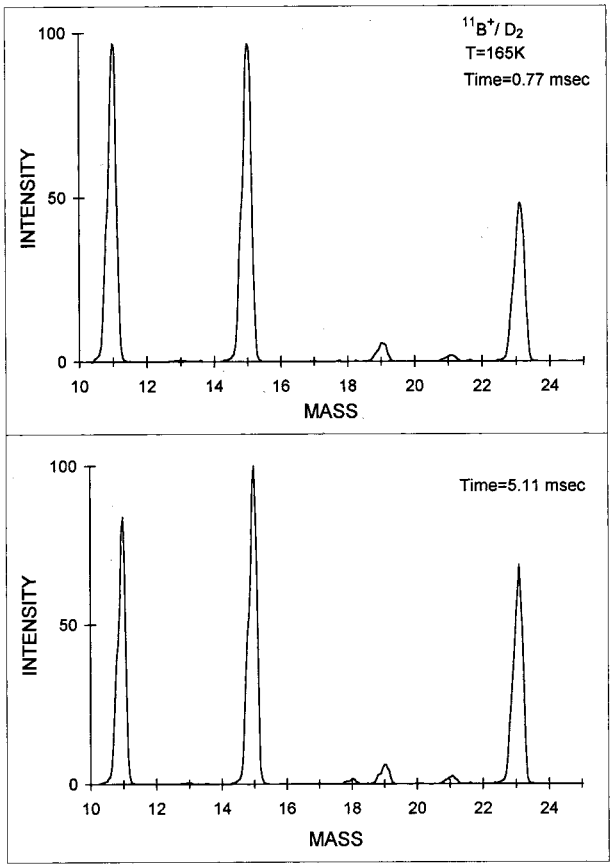

Figure 4. Mass spectra of ions exiting the drift reaction cell when $^{11}B^+$ was injected into 1.9 Torr of D_2 at 165 K. The top panel was for a drift time of 0.77 ms and the bottom panel for a drift time of 5.11 ms. In both cases the D_2 pressure was 1.9 Torr.

indicating these systems are in equilibrium. However, the $^{11}B^+(H_2)_3$ peak at $m/z = 17$ becomes larger as the drift time increases and totally dominates at $t = 7.36$ ms. Clearly this peak, of composition $^{11}BH_6^+$, is not in equilibrium with the remaining three peaks at lower mass, and represents the terminal ion formed from sequential H_2 addition to B^+.

A related set of data are given in Figure 4. In this instance $^{11}B^+$ ions react with D_2 at $T = 165$ K. Again equilibrium is established for addition of the first two D_2 molecules (although their intensities are lower due to the higher temperature). Now, however, there is only a minor increase in the terminal $^{11}BD_6^+$ ion as the time is increased by a factor of 20 from the top panel to the bottom panel, in sharp contrast to the 127 K results in Figure 3. These results were essentially independent of isotope used, $^{10}B^+$ or $^{11}B^+$, H_2 or D_2. A model that successfully explains these data will be presented in the Discussion Section.

Theory. High-level ab initio calculations were performed at the QCISD(T) level of theory[24] with use of a 6-311++G-(2df,p) basis set for both $B^+(H_2)_n$, for $n = 1$ to 6, and $HBH^+(H_2)_m$, for $m = 1$ and 2. Geometry optimizations were made at this level of theory except for $B^+(H_2)_n$ ($n = 3, 4, 5, 6$), where MP2 was used, followed by single-point calculations at QCISD-(T). Zero-point energy corrections were done at the Hartree−Fock SCF level of theory. These were compared to ZPE corrections calculated with use of MP2 for $B^+(H_2)_3$ and found to agree within 2%. These calculations are summarized in Table 2 where they are compared to experiment.

In recent years we have found density functional theory calculations to be very useful in the interpretation of experimental results for sequential binding of H_2 to transition metal ions.[11] In particular the Becke 3 parameter hybrid functional (B3LYP) has proven to provide relatively accurate binding energies for many systems and to be very informative about both metal orbital populations and $M^+(H_2)_n$ structures. We thought it useful to evaluate this method with a variety of basis sets on the systems studied here since both accurate experimental results and predictions of a very high level of ab initio calculations were available. We were also interested in exploring some of the potential surface of selected systems to try to rationalize the puzzling experimental results given in Figures 3 and 4. Such exploration is much easier to do with DFT methods.

The DFT calculations were done with the Dunning and Hay[25] (D95) double-ζ basis set, this same set with diffuse functions on all atoms (D95++), and this latter set with a variety of polarization functions (D95++(*n*d,*n*p)) or D95++(*n*df,*n*pd). These results were compared to Dunning's correlation consistent basis sets[26] augmented with diffuse functions and with double-ζ (AUG-cc-pVDZ), triple-ζ (AUG-cc-pVTZ), and quadruple-ζ (AUG-cc-pVQZ) quality. The results are given in Table 3 for $B^+(H_2)_n$ and in Table 4 for $HBH^+(H_2)_n$. The D95++(3df,3pd) results are also given in Table 2 for comparison with experiment and the QCISD(T) ab initio calculations. All calculations were done with use of the Gausian 94 package of programs.[27]

(24) Pople, J. A.; Head-Gordon, M.; Raghavachiri, K. *J. Chem. Phys.* **1987**, *87*, 5968.

(25) Dunning, T. H., Jr.; Hay, P. J. In *Modern Theoretical Chemistry*; Schaefer, H. F., III, Ed.; Plenum Press: New York, 1976; pp 1−28.

(26) Woon, D. E.; Dunning, T. H., Jr. *J. Chem. Phys.* **1993**, *98*, 1358. Kendall, R. A.; Dunning, T. H., Jr.; Harrison, R. J. *J. Chem. Phys.* **1992**, *96*, 6796. Dunning, T. H., Jr. *J. Chem. Phys.* **1989**, *90*, 1007.

Table 3. DFT(B3LYP) Binding Energies in kcal/mol for $B^+(H_2)_n$ Electrostatic Clusters for Various Basis Sets

n	basis set[a]	D_e	D_0
1	D95	5.91	5.56
	D95++	5.02	4.61
	D95++(d,p)	6.45	5.81
	D95++(2d,2p)	7.68	6.83
	D95++(3df,3pd)	7.62	6.82
	AUG-cc-pVDZ	8.93	8.01
	AUG-cc-pVTZ	7.77	6.95
	AUG-cc-pVQZ	7.78	
2	D95	5.12	4.11
	D95++	4.26	3.38
	D95++(d,p)	5.47	4.03
	D95++(2d,2p)	6.40	4.87
	D95++(3df,3pd)	6.33	4.97
	AUG-cc-pVTZ	6.44	4.98
3	D95++(d,p)	4.95	2.46
	D95++(2d,2p)	ca. 5.75[b]	
	D95++(3df,3pd)	ca. 5.79[b]	

[a] See text for description of basis sets. [b] Estimated, not a minimum with this basis set; see text.

Table 4. DFT(B3LYP) Binding Energies in kcal/mol for $HBH^+(H_2)_m$ Clusters for Various Basis Sets

m	basis set[a]	D_e	D_0
0[b]	D95	69.65	64.82
	D95++	68.68	63.84
	D95++(d,p)	71.49	66.75
	D95++(2d,2p)	71.52	66.94
	D95++(2df,2p)	72.17	67.59
	D95++(3df,3pd)	73.38	68.75
	AUG-cc-pVDZ	73.63	69.02
	AUG-cc-pVTZ	73.41	68.81
	AUG-cc-pVQZ	73.60	
1	D95++(d,p)	19.94	15.17
	D95++(2df,2p)	21.03	16.17
	D95++(3df,3pd)	21.10	16.18
2	D95++(2df,2p)	23.02	16.85
	D95++(3df,3pd)	23.54	17.35

[a] See text for basis set references. [b] This is the energy of the reaction $HBH^+ \rightarrow B^+(^1S, 2s^2) + H_2(^1\Sigma)$.

The data in Tables 2 and 3 indicate that the D95++(2d,2p) basis set gives results very close to the basis set limit, a useful[27] result since calculations with this basis are substantially cheaper than those with the cc-pVTZ basis. However, all basis sets substantially overestimate the H_2 binding energies (Table 2) with the greatest errors coming at the smallest sized cluster. The H−H bond lengths are substantially longer for B3LYP calculations than for either QCISD or MP2 in line with the increased bond energy.

One other point is worth mentioning. For the $B^+(H_2)_3$ system, basis sets larger than D95++(d,p) led to spontaneous insertion into one of the three H−H bonds leading to $HBH^+(H_2)_2$. We will come back to this point in the discussion section. Bound $B^+(H_2)_n$ minima were found with QCISD up to $n = 6$. No effort was made to determine barriers to insertion for $n = 3$ with QCISD.

(27) Gaussian 94, Revision C.2, Frische, M. J.; Trucks, G. W.; Schlegel, H. B.; Gill, P. M. W.; Johnson, B. G.; Robb, M. A.; Cheeseman, J. R.; Keith, T.; Peterson, G. A.; Montgomery, J. A.; Raghavachari, K.; Al-Laham, M. A.; Zakrzewski, V. G.; Ortiz, J. V.; Foresman, J. B.; Cioslowski, J.; Stefanov, B. B.; Nanayakkava, V. G.; Challacombe, M.; Peng, C. Y.; Syala, P. Y.; Chen, W.; Wong, M. W.; Andres, J. L.; Replogles, E. S.; Gomperts, R.; Martin, R. L.; Fox, D. J.; Binkley, J. S.; Defrees, D. J.; Baker, J.; Stewart, J. P.; Head-Gordon, M.; Gonzalez, C.; Pople, J. A., Gaussian Inc.: Pittsburgh, PA, 1995.

Discussion

Equilibrium Measurements. The addition of the first and second dihydrogen ligands to B^+ rapidly comes into equilibrium. These two H_2 molecules are weakly bound (3.8 and 3.0 kcal/mol, respectively), explaining why they were not observed in the flow tube measurements. The bonding in these systems is almost purely electrostatic. According to the QCISD(T) results the structure of $B^+(H_2)$ is C_{2v} as expected with B^+−H distances of 2.307 Å and an essentially unperturbed H−H distance of 0.756 Å. The H_2 bond axis is perpendicular to the B^+−H_2 bond axis to maximize the charge-quadrupole attraction. The second H_2 is added ∼90° to the first and rotated ∼90° from the plane the initial H_2 makes with B^+ leading to a structure of C_s symmetry. The third H_2 ligand adds ∼90° to the first two and the resulting ion is of C_3 symmetry. Similar structures were found in the weakly bound $Mn^+(4s^13d^5)$ and $Zn^+(4s^13d^{10})$ clusters with H_2.[28] In those instances electron repulsion between the M^+ 4s and the filled σ orbital on H_2 was mitigated by polarization of the 4s orbital by using the high-lying empty 4p orbitals to remove s-electron density from the M^+−H_2 bond axis. These orbitals also acted as (minor) acceptor orbitals for H_2 σ donation. The same mechanisms are probably at work here, although the double occupancy of the 2s orbital on B^+ and the high energy of the 3p orbitals reduce the effects somewhat.

The ab initio QCISD(T) calculations predict that up to 6 dihydrogen ligands can be attached to B^+ in the first solvation shell, eventually leading to a complex with octahedral symmetry. In contrast, the DFT calculations find a quite different result. The first two H_2 molecules are weakly bound. The third is bound only with the smallest basis set used. Larger basis sets lead to spontaneous insertion and formation of a $HBH^+(H_2)_2$ complex. More on this point later.

When HBH^+ ions were injected into the flow tube, sequential addition of two H_2 molecules occurred to form an $HBH^+(H_2)_2$ terminal ion.[19] This result was supported by ab initio calculations[19] that indicated the addition of two strongly bound H_2 ligands would occur. The first H_2 addition resulted in a planar C_{2v} complex with the H_2 ligand approaching the B^+ ion midway between the two H atoms and a theoretically predicted $D_0 =$ 14.5 kcal/mol. The second H_2 adds to form a quasi-tetrahedral complex (considering the H_2 ligands as single species) with a calculated $D_0 = 17.6$ kcal/mol. Our equilibrium results of 14.7 and 18.1 kcal/mol (Table 2) are thus in excellent agreement with these literature calculations as well as with our somewhat higher level calculations (Table 2). Our calculations find HBH^+ is linear, as expected, with an sp hybridized B^+ ion. Addition of the first H_2 leads to near sp^2 hybridization on B^+ and addition of the second H_2 to near sp^3 hybridization on B^+. The relatively strong bonds arise from three center two electron bonding between the H_2 ligands and the B^+ cluster.

B^+ Insertion into the H−H Bond. Simons and co-workers[17] have thoroughly investigated the B^+/H_2 potential surface using high-level ab initio methods. They found a weakly bound (1.2 kcal/mol) electrostatic B^+−H_2 complex in the entrance channel and a $^1\Sigma_g^+$ HBH^+ inserted species 42 kcal/mol below the B^+/H_2 asymptotic energy. Between was a transition state 77 kcal/mol above the asymptotic ground-state energy caused by the forbidden crossing of the states correlating to the $^1S_0$ ($2s^2$) ground state of B^+ and the ^1P (2s2p) first excited singlet state of B^+.

(28) Weis, P.; Kemper, P. R.; Bowers, M. T. *J. Phys. Chem. A* **1997**, *101*, 2809.

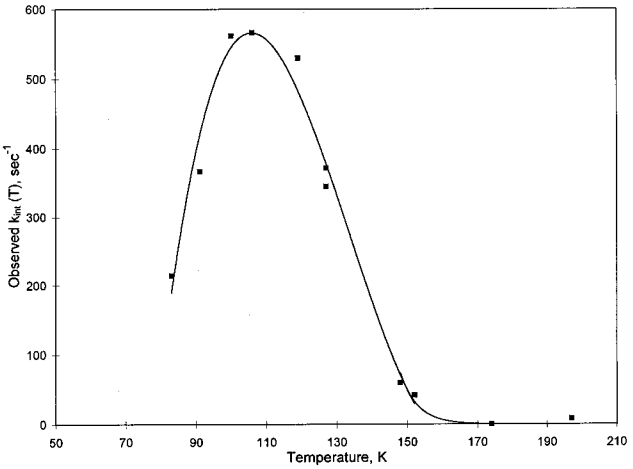

Figure 5. A plot of $k_{int}(T)$ vs temperature for reaction of $B^+(H_2)_n \rightarrow BH_6^+$. See text.

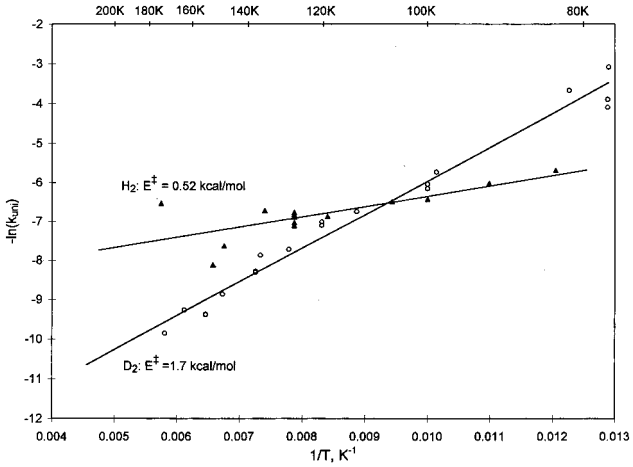

Figure 6. Plots of ln $k_{uni}(T)$ vs inverse temperature for $B^+(H_2)_3 \rightarrow HBH^+(H_2)_2$ and $B^+(D_2)_3 \rightarrow DBD^+(D_2)_2$. See text.

With these calculations in mind we initially assumed that ground-state B^+ ions would not insert into the H−H bond of H_2 no matter how many electrostatically bound H_2 molecules surrounded it. Hence, we were initially mystified when we saw data of the type presented in Figures 3 and 4. These data showed that the BH_6^+ species was a terminal ion and that its rate of formation was both time and temperature dependent. We were certain this species was not simply a "filled shell" $B^+(H_2)_3$ ion since, one, the ion was not in equilibrium with the other $B^+(H_2)_n$ ions, and, second, the very high level QCISD(T) calculations predicted a shell filling with 6 H_2 ligands. Instead, since BH_6^+ is the terminal ion when HBH^+ reacts with H_2, the inference is very strong that the stable BH_6^+ ion we observe is in fact $HBH^+(H_2)_2$.

Although complex kinetics must be present, the presence of equilibria greatly simplifies the analysis of the insertion reaction. First, all electrostatically (i.e. weakly) bound complexes are in rapid equilibrium under the experimental conditions employed. Hence

$$B^+ \underset{-H_2}{\overset{H_2}{\rightleftharpoons}} B^+(H_2) \underset{-H_2}{\overset{H_2}{\rightleftharpoons}} B^+(H_2)_2 \underset{-H_2}{\overset{H_2}{\rightleftharpoons}} B^+(H_2)_3 \underset{-H_2}{\overset{H_2}{\rightleftharpoons}} \ldots \quad (5)$$

It is clear that one of these species is the primary reactant forming the stable $HBH^+(H_2)_2$ ion. The assumption is then

$$B^+(H_2)_n \xrightarrow{k_{int}(T)} HBH^+(H_2)_2 + (n-3)H_2 \quad (6)$$

where $k_{int}(T)$ is the temperature-dependent insertion rate constant. In kinetic terms

$$I_n(t) = I_n(t=0)e^{-k_{int}(T)t} \quad (7)$$

where $I_n(t)$ is the observed intensity of the cluster $B^+(H_2)_n$ at time t. A plot of $\ln[I_n(t)/I_n(t=0)]$ versus t thus gives the value of $k_{int}(T)$ at the experimental temperature. It is important to note that this measured rate coefficient is independent of which electrostatic $B^+(H_2)_n$ cluster(s) is the actual reactant since all of the electrostatic complexes are in rapid equilibrium. Consequently, at any fixed temperature and fixed H_2 pressure the fractional abundances of all $B^+(H_2)_n$ clusters are independent of time. Thus for any value of n used in the measurement the same value of $k_{int}(T)$ (due to the loss process of reaction 6) will be observed. The resulting values of $k_{int}(T)$ are plotted versus T in Figure 5.

The plot of $k_{int}(T)$ vs temperature shows a quite unusual behavior. The observed rate maximizes near 100 K and decreases sharply to higher and lower temperatures. In a general view, this is due to an increasing concentration of the larger $B^+(H_2)_n$ clusters (one of which is the true reactant) as the temperature decreases, balanced against a decreasing reaction probability, due to a small barrier, as the temperature decreases. For a more specific explanation, we now convert our observed rate coefficient to true unimolecular rate constants, $k^n_{uni}(T)$ for the different $B^+(H_2)_n$ reactant clusters using

$$k^n_{uni}(T) = k_{int}(T)/f_n(T) \quad (8)$$

where f_n is the fraction of the particular $B^+(H_2)_n$ complex undergoing insertion. These rate coefficients are now independent of any $B^+(H_2)_n$ concentration. Using the Arrhenius equation for the barrier process we can write

$$k^n_{uni}(T) = Ae^{-E^‡RT} \quad (9)$$

where $E^‡$ is the insertion barrier for reaction 6. To determine which of the $B^+(H_2)_n$ clusters is the actual reactant we plot $-\ln[k^n_{uni}(T)]$ vs $1/T$ for all values of n and see which one gives a straight line. This was done, and a straight line was obtained only for $n = 3$ (Figure 6).

From this analysis we confirm that $k_{int}(T)$ decreases at $T >$ 100 K because the fraction of the third cluster decreases strongly above that temperature (Figure 5). The decrease in $k_{int}(T)$ below 100 K may be due to a small barrier of ∼0.5 kcal/mol. The experiments with D_2 gave essentially the same results, but with an increased barrier height of 1.7 kcal/mol (Figure 6). In summary, then, the proposed mechanism for formation of $HBH^+(H_2)_3$ from B^+ and nH_2 is

$$B^+ + 3H_2 \rightleftarrows B^+(H_2)_3 \xrightarrow{\Omega} HBH^+(H_2)_2 \quad (10)$$

It is almost certain that the nascent $HBH^+(H_2)_2$ ions formed in reaction 10 dissociate to form bare HBH^+ ions since reaction 10 is 55 kcal/mol exoergic. At the high H_2 pressures in the cell, however, the two H_2 ligands are rapidly reattached resulting in the observed BH_6^+ terminal ion.

We cannot rule out the possibility that a bimolecular reaction occurs between $B^+(H_2)_3$ and H_2 rather than the unimolecular reaction of $B^+(H_2)_3$ described above. An Arrhenius plot of the bimolecular rate coefficients gave nearly as good a straight line fit with derived activation energies of 0.7 (H_2) and 2.1 kcal/

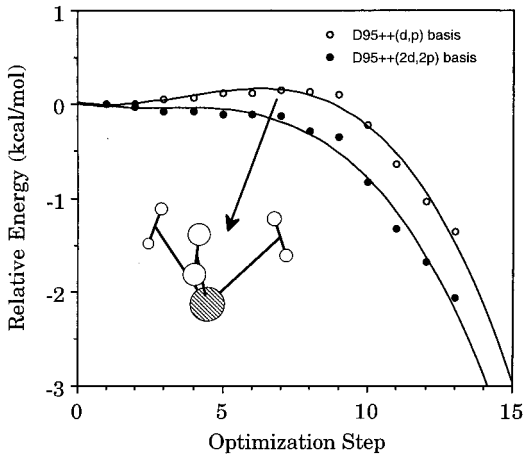

Figure 7. Theoretical energy optimization of the $B^+(H_2)_3$ complex showing the lack of activation energy for insertion. DFT calculations with two different basis sets are shown. The optimization steps shown are the individual geometry optimizations the calculation makes toward the lowest energy structure. Because there is little or no barrier, the optimization follows the reaction pathway to the inserted complex.

mol (D_2). The $E^{\ddagger}$ values for the two mechanisms are similar since the same fraction f_3 controls both rates. We favor the unimolecular mechanism since, as discussed below, calculations clearly show a low-energy pathway from $B^+(H_2)_3$ to $HBH^+(H_2)_2$. It is not obvious as how a fourth H_2 could aid the insertion process. This has been confirmed by detailed ab initio calculations.[29,30]

Although this mechanism does explain the experimental data, it has one apparent problem. As noted earlier, Simons and co-workers[17] had calculated a barrier of 77 kcal/mol for insertion on the $B^+(H_2)$ surface. It simply did not seem reasonable that adding two more H_2 ligands, bound by a total of about 5 kcal/mol, could possibly eliminate this barrier. We had earlier observed[12] that adding three weakly bound H_2 ligands to the 4s3d ^{3}D ground state of Sc^+ resulted in insertion into the H−H bond but in that case the barrier was only 17 kcal/mol[13,14] and the excited state correlating to inserted products only 31 kcal/mol above the ground state.[12] For the analogous B^+ reaction with a barrier of 77 kcal/mol and with the reactive excited state 207 kcal/mol above the ground state, it seemed unlikely that insertion could spontaneously occur at 100 K. None the less, we undertook high-level ab initio calculations to investigate the possibility. We were able to reproduce the B^+/H_2 minimum reaction path of Simons and co-workers;[17] however, we rapidly realized that adding two additional H_2 ligands greatly complicated the ab initio calculations and we chose to abandon this approach. (Fortunately, Prof. Greg Gellene took up the problem and successfully found the minimum energy reaction paths for B^+/H_2, $B^+(H_2)/H_2$, and $B^+(H_2)_2/H_2$ systems at the MP2/Aug-cc-pVTZ level of theory. This spectacular achievement is published in the paper following this one in the Journal.[29,30])

We did, however, continue our DFT calculations as previously mentioned. We noticed, to our surprise, that electrostatically bound $B^+(H_2)_3$ was a true minimum on the DFT potential surface only for the relatively small D95++(d,p) basis set. The use of larger basis sets ultimately led to spontaneous insertion. The minimum energy pathways in the region of the "transition state" for two basis sets are given in Figure 7. It is apparent that a very small, or zero, barrier is encountered to insertion at this level of theory. Our DTF calculations do not include zero-point energy effects, which raise the barrier by 3−4 kcal/mol according to Gellene's ab initio calculations.[29,30] The geometry we obtained for the "transition state" is given pictorially in Figure 7. The symmetry is C_{3v} and as the optimization step proceeds, the B^+ ion core moves from the top of the cylinder formed by the three H_2 ligands to a central position where it is essentially equidistant from all 6 H atoms. At this point the H−H distances are very large (∼1.0 Å) and the B^+ core simply slips between two of them while the remaining four H atoms retreat to reform two stable H_2 ligands. The final structure is essentially tetrahedral in shape (again, considering the H_2 ligands to be single species) and very similar to that calculated by high-level ab initio calculations (Table 2 and ref 19).

We were at first suspicious of these calculations, since they were single configuration and we assumed at least two configurations would be required (as was necessary for $B^+(H_2)$ insertion).[29] However, the ab initio calculations of Gellene[29,30] give a very similar picture, namely that insertion does in fact occur on the ground-state surface, indicating our DFT results are at least qualitatively correct. Detailed discussion of the process of insertion and the orbitals involved can be found in Gellene's ab initio paper.[29,30] One additional point is worth noting. It seems likely that our experimental activation energy does not result from surmounting a simple energy barrier but more likely from tunneling through a small barrier. The principal evidence for this is the calculated barrier height and isotope effect. The calculated barrier heights (including zero-point corrections) are 3.4 and 2.3 kcal/mol for H_2 and D_2 reactants, with respect to the separated reactants ($B^+(H_2)_2 + H_2$).[30] The barriers with respect to the stabilized $B^+(H_2/D_2)_3$ complexes are greater, 5.6 and 5.0 kcal/mol.[30] These are significantly greater than the experimental values of 0.52 and 1.7 kcal/mol. While these absolute values might be questioned, the *lower* relative size of the D_2 barrier is a robust result of the calculations, which is inconsistent with the experimental results. Both these disagreements between theory and experiment can be explained if the actual insertion process involves tunneling through a small barrier near the bottom of the $B^+(H_2/D_2)_3$ potential well. In this case, the experimental activation energies reflect the energy-dependent rate of tunneling (rather than the actual barrier height). Since the D_2 system is expected to show a slower rate, its apparent barrier height is larger, as we observe.

Conclusions

1. Binding energies of ground-state B^+ (^{1}S) ions with one and two H_2 ligands have been measured with use of equilibrium methods, with values of 3.8 and 3.0 kcal/mol obtained for D_0°, respectively. High-level ab initio calculations are in quantitative agreement with experiment and indicate the bonding is predominantly electrostatic.

2. Binding energies of HBH^+ ions with one and two H_2 ligands were also measured. In this case the ligands are much more strongly bound reflecting the sp^n hybrid character of the B^+ bonding orbitals. Again, excellent agreement is found with high-level ab initio calculations both from the literature[19] and from a somewhat higher level calculation reported here. The B^+-H_2 bonds in $HBH^+(H_2)$ and $HBH^+(H_2)_2$ can best be thought of as 2 electron 3 center bonds.

3. Kinetic evidence is given for the cluster assisted, facile insertion of ground-state B^+ into H_2. Analysis of the data indicates it is most likely $B^+(H_2)_3$ that spontaneously inserts forming $HBH^+(H_2)_2$. This process proceeds with essentially no barrier at 100 K despite the fact that insertion of isolated

(29) Gellene, G.; Proceedings of the 45th ASMS Conference on Mass Spectrometry & Allied Topics.

(30) Gellene, G. *J. Am. Chem. Soc.* **1998**, *120*, 7585.

ground-state B^+ ions into H_2 must surmount a 77 kcal/mol barrier. The key is that $B^+(H_2)_3$ can remain on the ground-state surface during insertion. However, for the isolated ^1S ($1s^2$ $2s^2$) ground-state B^+ ions to insert into the H−H bond of a single H_2 molecule, the ion must undergo a forbidden crossing with a state correlating to the high-lying ^1P ($1s^2$ 2s2p) state of B^+.

4. Large basis set DFT calculations were performed. The H_2 binding energies for the weakly bound $B^+-(H_2)$ and $B^+(H_2)-(H_2)$ clusters were overestimated by about a factor of 2 compared to either experiment or high-level ab initio calculations (Table 2). Better agreement was obtained with experiment for the much more strongly bound $HBH^+-(H_2)$ and $HBH(H_2)^+-(H_2)$ systems. The DFT calculations did predict that $B^+(H_2)_3$ should insert with little or no barrier to form $HBH(H_2)_2^+$ in agreement with experiment. These single configuration calculations support the view that the insertion process occurs solely on the ground-state surface, as indicated by high-level ab initio calculations reported elsewhere.[29,30]

Acknowledgment. We gratefully acknowledge the support of the National Science Foundation under Grant No. CHE-9729146 and the partial support of the Air Force Office of Scientific Research under grants F49620-96-1-0033 and F49620-96-1-0247. Useful conversations with and receipts of results prior to publication from, Prof. Greg Gellene are also gratefully acknowledged. Finally we thank Prof. Chuck DePuy for getting us interested in the problem.

JA9739751